International Journal of Phytoremediation

ISSN: 1522-6514 (Print) 1549-7879 (Online) Journal homepage: http://www.tandfonline.com/loi/bijp20

Utilization of unconventional lignocellulosic waste biomass for the biosorption of toxic triphenylmethane dye malachite green from aqueous solution

Rangabhashiyam Selvasembian & Balasubramanian P

To cite this article: Rangabhashiyam Selvasembian & Balasubramanian P (2018) Utilization of unconventional lignocellulosic waste biomass for the biosorption of toxic triphenylmethane dye malachite green from aqueous solution, International Journal of Phytoremediation, 20:6, 624-633, DOI: 10.1080/15226514.2017.1413329

To link to this article: https://doi.org/10.1080/15226514.2017.1413329

Published online: 24 Apr 2018.

INTERNATIONAL JOURNAL OF PHYTOREMEDIATION
2018, VOL. 20, NO. 6, 624–633
https://doi.org/10.1080/15226514.2017.1413329

Taylor & Francis
Taylor & Francis Group

Utilization of unconventional lignocellulosic waste biomass for the biosorption of toxic triphenylmethane dye malachite green from aqueous solution

Rangabhashiyam Selvasembian and Balasubramanian P

Department of Biotechnology and Medical Engineering, National Institute of Technology, Rourkela, Odisha, India

ABSTRACT

Biosorption potential of novel lignocellulosic biosorbents Musa sp. peel (MSP) and *Aegle marmelos* shell (AMS) was investigated for the removal of toxic triphenylmethane dye malachite green (MG), from aqueous solution. Batch experiments were performed to study the biosorption characteristics of malachite green onto lignocellulosic biosorbents as a function of initial solution pH, initial malachite green concentration, biosorbents dosage, and temperature. Biosorption equilibrium data were fitted to two and three parameters isotherm models. Three-parameter isotherm models better described the equilibrium data. The maximum monolayer biosorption capacities obtained using the Langmuir model for MG removal using MSP and AMS was 47.61 and 18.86 mg/g, respectively. The biosorption kinetic data were analyzed using pseudo-first-order, pseudo-second-order, Elovich and intraparticle diffusion models. The pseudo-second-order kinetic model best fitted the experimental data, indicated the MG biosorption using MSP and AMS as chemisorption process. The removal of MG using AMS was found as highly dependent on the process temperature. The removal efficiency of MG showed declined effect at the higher concentrations of NaCl and $CaCl_2$. The regeneration test of the biosorbents toward MG removal was successful up to three cycles.

KEYWORDS

Aegle marmelos shell; biosorption isotherm models; biosorption; malachite green; Musa sp. peel

Introduction

Malachite Green (MG) is a synthetic cationic dye belongs to category of triphenylmethane and associated with the property of highly water soluble. MG widely used to control fungal attacks protozoan infections in the aquaculture, as disinfectant in fish farming industry and animal husbandry, as an antiseptic and fungicidal reagent in humans (Lin and Chang 2015). MG finds its applications in the industrial sectors of dyeing cotton, silk, wool, paper, and leather (Elhalil *et al.* 2016). Despite the extensive use of MG in industrial applications and medical field, MG causes harmful effects on human health and environmental damages. The hazardous impacts of MG include carcinogenesis, mutagenesis, teratogenesis, cause respiratory diseases, damage the immune, reproductive and nervous systems (Srivastava *et al.* 2004; Shirmardi *et al.* 2013). Moreover, the MG discharge into the hydrosphere produces perceptible coloration even at low MG concentration due to its higher tinctorial value, reduces penetration of sunlight and affects the photosynthetic activity (Liu *et al.* 2017; Adel and Nasser 2016). Therefore, there is a growing concern for the removal of MG from industrial effluents before discharge into the water environment.

The conventional treatment methods (Mustafa *et al.* 2014) for the removal of synthetic dyes from the industrial wastewater were performed through the chemical (oxidative, fenton, photocatalytic, electrochemical) (Bandala *et al.* 2008; Zhou *et al.* 2015), biological (white-rot fungi, mixed microbial cultures, microbial enzymes, living/dead microbial biomass) (Zeng *et al.* 2015; Kumar *et al.* 2013; Rangabhashiyam *et al.* 2013a) and physical (adsorption by activated carbon, membrane filtration, ion exchange, irradiation, electrokinetic coagulation) (Alventosa-de Lara *et al.* 2012; Amin 2008). However, these conventional effluent treatment methods are not economical, constrain in power management, methodologically demanding and generate concentrated toxic sludge (Mustafa *et al.* 2014; Rangabhashiyam *et al.* 2013b). In the recent years, biosorption emerged as an alternative potential method over the conventional treatment process with the merits of efficient removal even at very low dye concentrations, environmental friendliness, cheaper, ease of operation, and consistent performance (Vijayaraghavan *et al.* 2017; Rangabhashiyam *et al.* 2017). The strategies for the biosorbent selection include low cost with little need of processing, abundantly distributed natural residues or by-product/waste material from the agricultural practice (Rangabhashiyam *et al.* 2014a). Most of the explored lignocellulosic biomass toward MG removal from aqueous solutions demonstrated with lower biosorption capacity, which may not be sufficient for the replacement of commercially available expensive activated carbon. Therefore, the hunt toward the seeking of novel lignocellulosic biosorbents is continuing.

To the best of our knowledge, the removal of MG as a model pollutant has not been investigated yet using MSP and AMS biosorbents. The present research carried out with the following objectives: to perform characterization of MSP and AMS

CONTACT Rangabhashiyam Selvasembian rambhashiyam@gmail.com; Balasubramanian P biobala@nitrkl.ac.in Biotechnology and Medical Engineering, National Institute of Technology Rourkela, Odisha 769 008, India.

Color versions of one or more of the figures in the article can be found online at www.tandfonline.com/bijp.

using Field Emission Scanning Electron Microscopy (FE-SEM), X-ray Diffractometer (XRD) and Fourier transform infrared spectroscopy (FT-IR). To study the effect of initial pH, biosorbent dosage, initial MG concentration and temperature on the MG biosorption. To analyze the experimental data with two, three parameters isotherm and kinetic models, followed with thermodynamic investigations. To perform the biosorbent regeneration using the desorbing agents. To evaluate the influence of salt ionic strength on the MG biosorption process.

Materials and methods

Biosorbents preparation

The biomass of the Musa sp. peel and Aegle marmelos shell were obtained from a local fruit stall at Rourkela, India. The biomass was washed thoroughly with distilled water and further oven dried at 383 K for 24 h to remove the moisture content. The dried biomass was ground to fine powder using a blender, sorted using standard test sieves in the fraction range of 100–200 μm and termed as Musa sp. peel (MSP) and Aegle marmelos shell (AMS). The prepared biosorbents were used for the dye biosorption studies without any additional chemical or physical treatments.

Preparation of aqueous dye solutions

The stock solution of the basic dye malachite green (C.I. 42000; Basic Green 4 and chemical formula $C_{23}H_{25}ClN_2$) was prepared by dissolving appropriate amount of malachite green in the distilled water. The chemicals utilized in this study were of analytical grade reagents and used without further purifications. Samples of the working solutions for each experiment were prepared by dilution of malachite green (MG) stock solution with distilled water to the required concentrations. The initial pH of the aqueous MG solutions was adjusted with 0.1 M HCl and 0.1 M NaOH solutions. The calibration curve for MG was prepared in the concentration range of 0–10 mg/L, measured spectrophotometrically at 619 nm.

Biosorbents characterization

The surface characteristics of the biosorbent samples were examined by Field Emission Scanning Electron Microscopy (FE-SEM) Quanta 250 FEG. The X-ray diffraction (XRD) measurements of biosorbents were conducted using Rigaku Ultima-IV. The active functional group on the surface of biosorbents was determined using Fourier transform infrared spectroscopy (FT-IR) analysis done using Perkin Elmer Spectrum Two. 2.4.

Method of experiments

Batch biosorption experiments were carried out to study the effect of parameters like initial solution pH, initial MG concentration, biosorbents dosage and temperature, at a constant agitation speed of 120 rpm. MG biosorption using MAP and AMS was carried out in 250 mL stoppered conical flasks containing 50 mL of known concentrations of MG solution and necessary amount of the biosorbent. The time required to attain the equilibrium for the dye biosorption was estimated through withdrawing of samples at regular time intervals till the equilibrium condition reached. At the fixed time intervals, residual concentration of the MG was analyzed through double beam UV–visible spectrophotometer (Systronics 2203). All the biosorption experiments were carried out in duplicates and the average values were recorded. The biosorption capacities of MSP and AMS toward the removal of MG were calculated using the following mass balance equation

$$q_e = \frac{(C_0 - C_e)}{m} \times V \tag{1}$$

where q_e is the equilibrium biosorption capacity (mg/g), C_0 and C_e are the initial and equilibrium concentration of MG in solution (mg/L), m represent the mass of biosorbent (g) and V indicate the volume of MG solution (L).

The MG removal percentage was determined using the following equation:

$$\%\ \text{Removal} = \left(\frac{C_0 - C_e}{C_0}\right) \times 100 \tag{2}$$

The effect of ionic strength on the biosorption of MG onto MAP and AMS was investigated with the addition of NaCl and $CaCl_2$ concentration range from 0.01 to 0.5 mol/L to the biosorption medium. For the biosorbent regeneration study, the dye loaded biosorbent was contacted with the desorbing agents (0.1 M HCl, 0.1 M H_2SO_4) and the experimental conditions for the desorption process are followed similar to that of the batch biosorption process. The biosorbent after the desorption process was subjected to wash with distilled water and dried in oven. The regenerated biosorbent was tested for the reusability studies by repeating the biosorption process followed with the desorption up to three cycles.

Biosorption isotherm and kinetic studies

In order to examine the relationship between biosorbed and aqueous concentration of dye at equilibrium condition, it is vital to establish the most appropriate correlations. The equilibrium biosorption isotherms are fundamental in describing the interactive behavior between biosorbate and biosorbent, which is important to optimize the design of the biosorption system (Rangabhashiyam *et al.* 2014b). The biosorption isotherm studies were conducted by varying the initial MG concentration at a constant biosorbent dosage under equilibrium condition. In the present study, the equilibrium biosorption data were fitted with two parameters isotherm models like Langmuir (Langmuir 1918), Freundlich (Freundlich 1906), Jovanovic (Jovanovic 1969), Halsey (Halsey 1948) and three parameter isotherm such as Redlich–Peterson (Redlich and Peterson 1959), Koble–Corrigan (Koble and Corrigan 1952), and Sips (Sips 1948) respectively. The expressions of the nonlinear forms of two and three parameter biosorption isotherm models are presented in Table 1.

The dye biosorption onto biosorbent materials is a complex process due to the heterogeneity nature of biosorbent surface. The biosorbate residence time is an important factor with

Table 1. The nonlinear forms of two and three parameter biosorption isotherm models.

Isotherm models	Equations	
Langmuir	$q_e = \frac{Q_0 K_L C_e}{1 + K_L C_e}$	(3)
Freundlich	$q_e = {}^{e}K_F C_e^{1/n_F}$	(4)
Jovanovic	$q_e = q_{mj}\left(1 - e^{(K_j C_e)}\right)$	(5)
Halsey	$q_e = \exp\left(\frac{\ln K_H - \ln C_e}{n_H}\right)$	(6)
Redlich–Peterson	$q_e = \frac{A_{RP} C_e}{1 + B_{RP} C_e^g}$	(7)
Koble–Corrigan	$q_e = \frac{A_{KC} C_e^n}{1 + B_{KC} C_e^n}$	(8)
Sips	$q_e = \frac{q_{m_s} K_S C_e^{m_s}}{1 + K_S C_e^{m_s}}$	(9)

Table 2. The expressions of biosorption kinetic models.

Kinetic models	Equations	
Pseudo-first-order	$\frac{dq_t}{dt} = k_1(q_e - q_t)$	(10)
Pseudo-second-order	$\frac{dq_t}{dt} = k_2(q_e - q_t)^2$	(11)
Elovich	$\frac{dq_t}{dt} = \alpha \exp(-\beta q_t)$	(12)
Intraparticle diffusion	$q_t = k_{id} t^{1/2} + C$	(13)

respect to the aspect of biosorption rate, since it has the influence on the solid–liquid interface. Kinetic model analysis of the experimental data useful to understand the controlling mechanism of dye biosorption processes. Biosorption kinetic studies were carried out at a fixed biosorbent dosage with varying initial MG concentration and contact time. Four biosorption kinetic models, including pseudo-first-order kinetic (Lagergren 1898), pseudo-second-order kinetic (Ho and McKay 1999), Elovich (Wu et al. 2009), and Intraparticle diffusion models (Weber and Morris 1962) were employed to evaluate the experimental data of MG biosorption onto MSP and AMS. The expressions of biosorption kinetic models are represented in Table 2.

Results and discussion

Characterization of MSP and AMS

The FE-SEM analysis enables the direct observation of the surface microstructures of MSP and AMS. The FE-SEM image of MSP (Fig. 1a) showed rough and undulated surface with little pores present on the biosorbent. Figure 1b represented FE-SEM image of AMS revealed that the texture of the biosorbent surface distributed with several macropore structure. The presence of such morphology in MSP and AMS offers the increased exposure of the biosorption active sites for the accessibility of MG to the biosorbent surface and favors higher dye removal efficiency.

XRD characterization used to analyze whether the biosorbent is crystalline or amorphous in nature. The two diffraction peaks observed around the 2 Theta positions of 17 and 22 in the native form of MSP and AMS. The XRD pattern of MPS and AMS confirmed the occurrence of cellulosic constituent in the biosorbents (Kaur and Kaur 2017). Significant difference in the XRD patterns were found in the MG loaded MPS and AMS compared to the native biosorbents. The difference in the intensity and 2 Theta position in the dye interacted biosorbents suggested that the MG after biosorption onto the MPS and AMS might induced the bulk phase changes in the biosorbents.

The involvement of the biosorbent functional groups in the removal of MG from aqueous solutions was examined using the characterization technique of FT-IR spectroscopy analysis. Figure 3a and 3b shows the FT-IR spectra of MSP, MG loaded MSP and AMS, MG loaded AMS respectively. The FT-IR spectra MSP and AMS displayed more number of absorption peaks; demonstrated the complex nature of the biosorbents. The FT-IR spectra of the biosorbents before and after MG biosorption were recorded in the wave number range of 400–4000 cm^{-1}. The FT-IR bands of MSP at 3380 and 2926 cm^{-1} were assigned to the functional groups of OH stretching and C–H stretching of alkane. The band position at 1612 cm^{-1} specified the aromatic skeleton vibrations of lignin fraction from MSP and shifted to 1626 cm^{-1} in the MG loaded MSP.

The peak at 1384 cm^{-1} was assigned to symmetrical stretching vibrations of NO_2 functional groups or because of the bending vibrations of CH_3 and COO– functional groups, this peak transformed into a number of smaller peak positions in case of MG loaded MSP signified the MG interaction. A minor band from 1060 to 1036 cm^{-1} was attributed to the C–O stretching vibrations of primary alcohol (Tzvetkov *et al.* 2016; Wang 2010). The OH stretching vibration of native AMS and MG

Table 3. Thermodynamic parameters for the MG removal using MSP and AMS at different initial concentrations.

Initial MG concentration (mg/L)	Temperature (K)	MSP			AMS		
		ΔG° (kJ/mol)	ΔH° (kJ/mol)	ΔS° (J/mol K)	ΔG° (kJ/mol)	ΔH° (kJ/mol)	ΔS° (J/mol K)
10	303	−5.62	11.45	56.50	−5.53	4.21	32.12
	313	−6.30			−5.82		
	323	−6.74			−6.17		
20	303	−5.16	12.82	59.53	−3.91	22.15	85.96
	313	−5.90			−4.69		
	323	−6.34			−5.64		
30	303	−4.88	10.90	52.07	−3.05	30.07	109.16
	313	−5.36			−3.92		
	323	−5.92			−5.25		
40	303	−4.50	13.81	60.56	−2.12	32.88	114.81
	313	−5.20			−2.62		
	323	−5.70			−4.44		
50	303	−4.14	8.60	42.07	−7.71	31.96	108.16
	313	−4.56			−1.97		
	323	−4.98			−2.93		

Table 4. The isotherm model parameters obtained for MG biosorption onto MSP and AMS.

Isotherm models	Parameters	MSP	Coefficient of determination (R^2)	AMS	Coefficient of determination (R^2)
Langmuir	Q_0 (mg/g)	47.61	0.994	18.86	0.996
	K_L (L/mg)	0.2121		0.4907	
Freundlich	K_F (L/g)	7.99	0.996	6.039	0.978
	n_F	1.3642		2.2831	
Jovanovic	q_{mj} (mg/g)	5.21	0.873	5.87	0.685
	K_j (L/g)	−0.163		−0.044	
Halsey	K_H	0.0584	0.996	0.01645	0.978
	n_H	−1.3642		−2.2831	
Redlich–Peterson	A_{RP} (L/g)	11.85	0.998	12.83	0.993
	B_{RP} (L/mg)^g	0.44		0.95	
	g	0.713		0.891	
Koble–Corrigan	A_{KC} (mg/g) (L/mg)^n	7.51	0.998	9.09	0.996
	B_{KC} (L/mg)^n	−0.02		0.41	
	n	0.737		0.768	
Sips	q_{mS} (mg/g)	111.11	0.999	23.80	0.998
	K_S (L/mg)^{mS}	0.0789		2.7857	
	m_S	0.835		0.721	

loaded AMS were observed at 3360 and 3484 cm^{-1}, respectively. The band shift of about 24 cm^{-1} was observed might be due to hydrogen bonding between the OH group of AMS and malachite green. The FT-IR spectra of AMS at the band positions of 2919, 1737, 1506, and 1426 cm^{-1} does not showed remarkable shift in band position in the MG interacted AMS. The band position of AMS at 1247 cm^{-1} represents the stretching vibration of C–N functional group, and shifted to 1260 cm^{-1} in the MG loaded AMS. The FT-IR spectra analysis of MSP and AMS indicated the occurrence of distinct functional groups and offered potential interaction sites for the MG biosorption.

Table 5. The kinetic model parameters for MG biosorption onto MSP and AMS at different initial concentrations.

Kinetic models	Parameters	Values				
				MSP		
Pseudo-first-order	C_0 (mg/L)	10	20	30	40	50
	k_1 (1/min)	0.0299	0.0414	0.0437	0.0345	0.0368
	q_e (mg/g)	1.5631	2.5118	4.9888	6.0394	7.1779
	R^2	0.712	0.846	0.849	0.828	0.896
				AMS		
	k_1(1/min)	0.0230	0.0322	0.0345	0.0322	0.0299
	q_e (mg/g)	1.2823	1.8379	6.6221	6.6527	6.1094
	R^2	0.800	0.860	0.861	0.903	0.899
Pseudo-second-order				MSP		
	C_0 (mg/L)	10	20	30	40	50
	k_2 (g/mg min)	0.0656	0.0648	0.0288	0.0196	0.0174
	q_e (mg/g)	4.8076	9.5238	14.2857	18.8679	23.2558
	R^2	0.998	0.999	0.999	0.999	0.999
				AMS		
	k_2(g/mg min)	0.0644	0.0342	0.0130	0.0124	0.0144
	q_e (mg/g)	4.0485	7.8125	11.6279	14.7058	16.3934
	R^2	0.999	0.999	0.998	0.999	0.999
Elovich				MSP		
	C_0 (mg/L)	10	20	30	40	50
	α (mg/g min)	3.29×10^6	6.27×10^{10}	0.10×10^9	5.18×10^6	3.42×10^6
	β (g/mg)	4.5871	3.2894	1.7064	1.1111	0.8643
	R^2	0.903	0.975	0.971	0.983	0.983
				AMS		
	α (mg/g min)	2.99×10^3	4.92×10^3	235.55	452.66	3714.60
	β (g/mg)	3.5842	1.8248	0.9319	0.7593	0.8077
	R^2	0.969	0.960	0.982	0.993	0.988
Intraparticle diffusion				MSP		
	C_0 (mg/L)	10	20	30	40	50
	k_{id} (mg/g min$^{1/2}$)	0.064	0.087	0.173	0.261	0.329
	C (mg/g)	3.961	8.443	12.07	15.53	19.24
	R^2	0.915	0.918	0.972	0.949	0.914
				AMS		
	k_{id} (mg/g min$^{1/2}$)	0.079	0.155	0.317	0.379	0.353
	C (mg/g)	3.073	5.944	7.555	9.941	12.04
	R^2	0.901	0.885	0.984	0.944	0.926

Nomenclature	
q_e	Equilibrium dye concentration on biosorbent (mg/g)
C_0	Initial dye concentration in aqueous solution (mg/L)
C_e	Equilibrium dye concentration in aqueous solution (mg/L)
V	Volume of the dye solution (L)
m	Mass of the biosorbent (g)
R^2	Coefficient of determination
Q_0	Biosorption capacity from Langmuir isotherm (mg/g)
K_L	Langmuir constant related to energy (L/mg)
K_F	Freundlich isotherm constant (L/g)
n_F	Freundlich heterogeneity factor
q_{mj}	Maximum biosorption capacity from Jovanovic isotherm (mg/g)
K_j	Jovanovic isotherm constant (L/g)
K_H	Halsey isotherm model constant
n_H	Halsey isotherm model exponent
A_{RP}	Redlich–Peterson model constant (L/g)
B_{RP}	Redlich–Peterson model constant $(L/mg)^g$
G	Redlich–Peterson model exponent
A_{KC}	Koble–Corrigan model constant (mg/g) $(L/mg)^n$
B_{KC}	Koble–Corrigan model constant $(L/mg)^n$
N	Koble–Corrigan model exponent
q_{ms}	Maximum biosorption capacity from Sips isotherm (mg/g)
K_s	Sips model constant $(L/mg)^{ms}$
m_s	Sips model exponent
k_1	Pseudo-first-order kinetic model rate constant (1/min)
k_2	Pseudo-second-order kinetic model rate constant (g/mg min)
A	Initial rate of biosorption (mg/g min)
B	Elovich constant (g/mg)
k_{id}	Intraparticle diffusion model constant $(mg/g\ min^{1/2})$
C	Boundary layer thickness (mg/g)
ΔG°	Gibbs free energy change (kJ/mol)
ΔH°	Enthalpy change (kJ/mol)
ΔS°	Entropy change (J/mol K)

Effect of pH on MG removal

The initial pH of the biosorption medium is a significant parameter in the dye removal performance. The effect of the initial solution pH on MG biosorption was studied over the pH range of 2.0 to 10.0 (Fig. 4a) at the initial MG concentration of 10 mg/L. The minimum biosorption capacity of MSP toward MG removal was observed at the initial pH 2.0 and increased with an increase of the initial pH up to 7.0 and then remains almost constant over the initial pH ranges from 7.0 to 10.0. For the biosorption of MG using AMS, the maximum biosorption capacity of 3.98 mg/g was observed at the initial pH of 8.0. The results show that the solution pH has direct influence over the MG biosorption process. At the low pH condition, more H^+ ions will exist in the biosorption medium, leads to the competition effect by electrostatic repulsion with cationic MG dye for the biosorption site. At the higher solution pH, the surface of MSP and AMS become negatively charged favors higher MG removal through electrostatic force of attraction (Sushmita *et al.* 2016). The value of the point of zero charge of MSP and AMS were determined as 6.70 and 6.20. The biosorbent surface was positively charged at the value of pH lesser than point of zero charge. For the further biosorption experiments, optimum initial pH of 7.0 (MSP) and 8.0 (AMS) were used for the removal of MG from aqueous solutions.

Effect of biosorbent dosage on MG removal

The influence of MSP and AMS dosage on the removal of MG was studied using biosorbent dosage range of 0.02–0.18 g with 10 mg/L initial MG concentration. The results of the biosorption capacity and the percentage removal of MG for the various biosorbent dosages were presented in Figure 4b. The percentage removal of MG increased from 87.18 to 94.91% (MSP) and from 79.46 to 95.56% (AMS) for the biosorbent dosage increase from 0.02 g to 0.1 g (MSP) and from 0.02 to 0.12 g (AMS). The percentage MG removal remained almost constant beyond the further increase of the biosorbents dosage of 0.1 g (MSP) and 0.12 g (AMS). Whereas, the biosorption capacity toward MG removal by both the biosorbents showed opposite trend. For the increase of biosorbent dosage value from 0.02 to 0.18 g, the biosorption capacity of MSP and AMS showed decreased effect from 21.79 to 2.63 mg/g and from 19.86 to 2.64 mg/g, respectively. The results of the increased percentage removal of MG are due to the higher biosorbent surface area and increased biosorption sites. The decrease in the biosorption capacity was attributed to the biosorbed dye onto unit mass of the biosorbent get split with increase of the biosorbent dosage at fixed dye concentration (Rajesh Kannan *et al.* 2010).

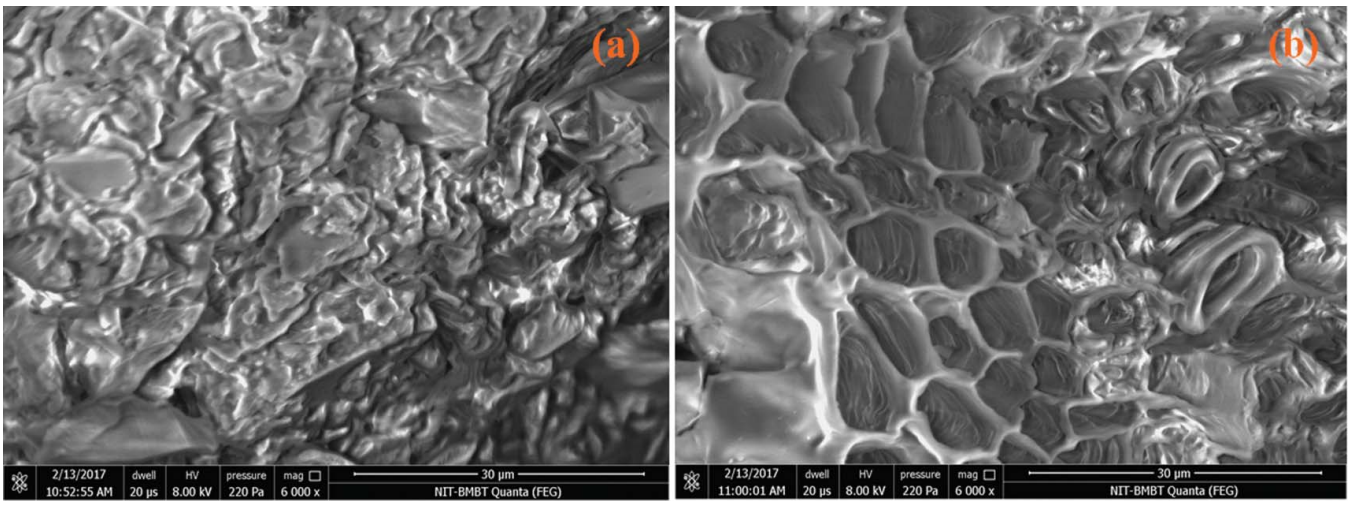

Figure 1. FE-SEM images of (a) MSP and (b) AMS.

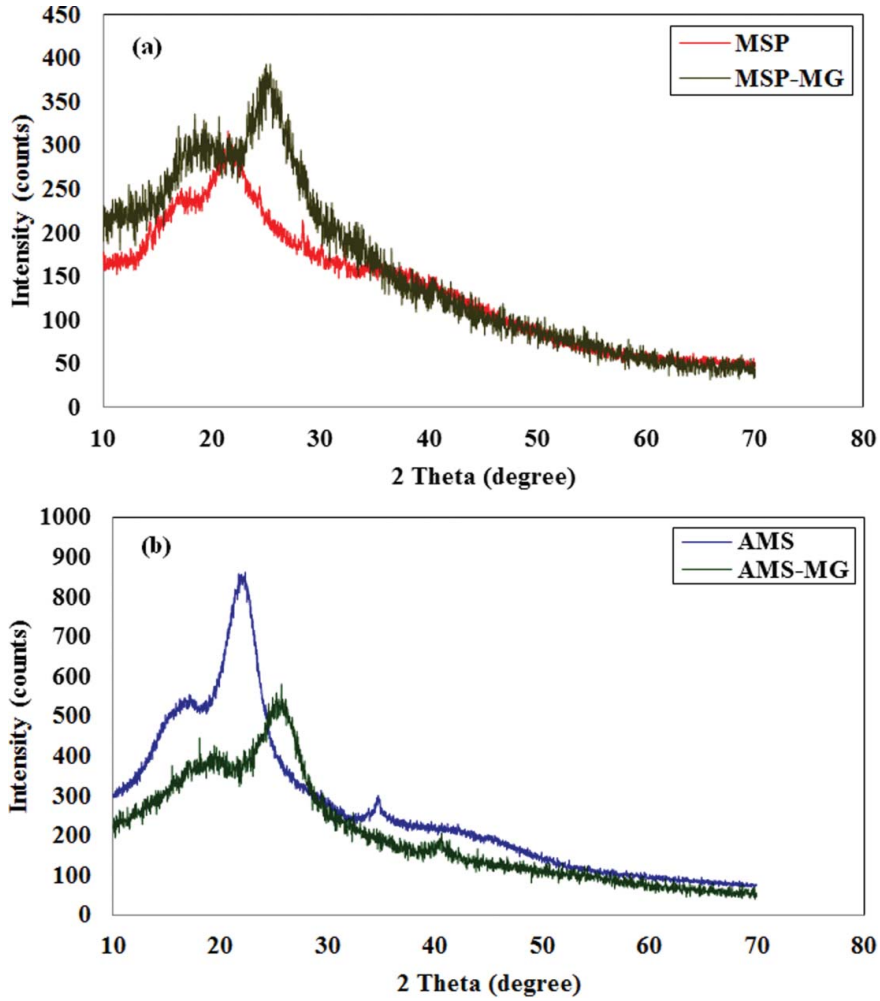

Figure 2. XRD patterns of (a) MSP, MG-loaded MSP and (b) AMS, MG-loaded AMS.

Effect of contact time and initial MG concentration on dye removal

The biosorption experiments for different contact time in the initial MG concentration range from 10 to 50 mg/L concentration were studied. The maximum biosorption capacity was occurred nearly at 140 min for MSP and AMS (figure not shown), this time was considered as the equilibrium time for the biosorption investigations. The effect of initial MG concentration on the biosorption capacity of MSP and AMS towards MG removal was illustrated in Figure 4c. With an increase of initial dye concentration increased from 10 to 50 mg/L, the biosorption capacities of MSP and AMS increased from 4.74 to 22.79 mg/g and 3.98 to 15.94 mg/g, respectively. The initial concentration of MG in the biosorption medium offers the essential driving force in order to overcome the MG mass transfer resistance between the biosorbent phase and the aqueous phase (Dahri *et al.* 2015). The enhanced driving force of the concentration gradient was exhibited with the increase of initial MG concentration.

Effect of temperature on MG removal

The examination on the effect of solution temperature on the percentage removal of MG was conducted at various initial MG concentrations and the results obtained were presented in Figure 4d. The results indicated that the percentage removal of MG using MSP was slightly increased with the increases in temperature from 303 to 323 K for all the initial concentrations of MG. The MG biosorption using AMS showed higher percentage removal with the solution temperature increase for 20 to 100 mg/L initial MG concentration. The results revealed that at the higher temperature, MG has adequate energy for biosorbent interaction and enhance the diffusion rate of MG by decrease of the viscosity of biosorption medium (Fumihiko *et al.* 2015).

Table 3 presents the calculated thermodynamic parameter values of the MG biosorption using MSP and AMS performed at different initial concentrations. The spontaneous nature of MG biosorption was appeared due to negative values of the Gibbs free energy change (ΔG°). The enthalpy change (ΔH°) values were found positive, indicated the endothermic nature of interaction between MG and biosorbents. The positive values of entropy change (ΔS°) represented the increase in degree of freedom of the biosorbed MG molecules.

Equilibrium biosorption modeling

The biosorption isotherm model constants of two and three parameters, along with the coefficient of determination (R^2) for

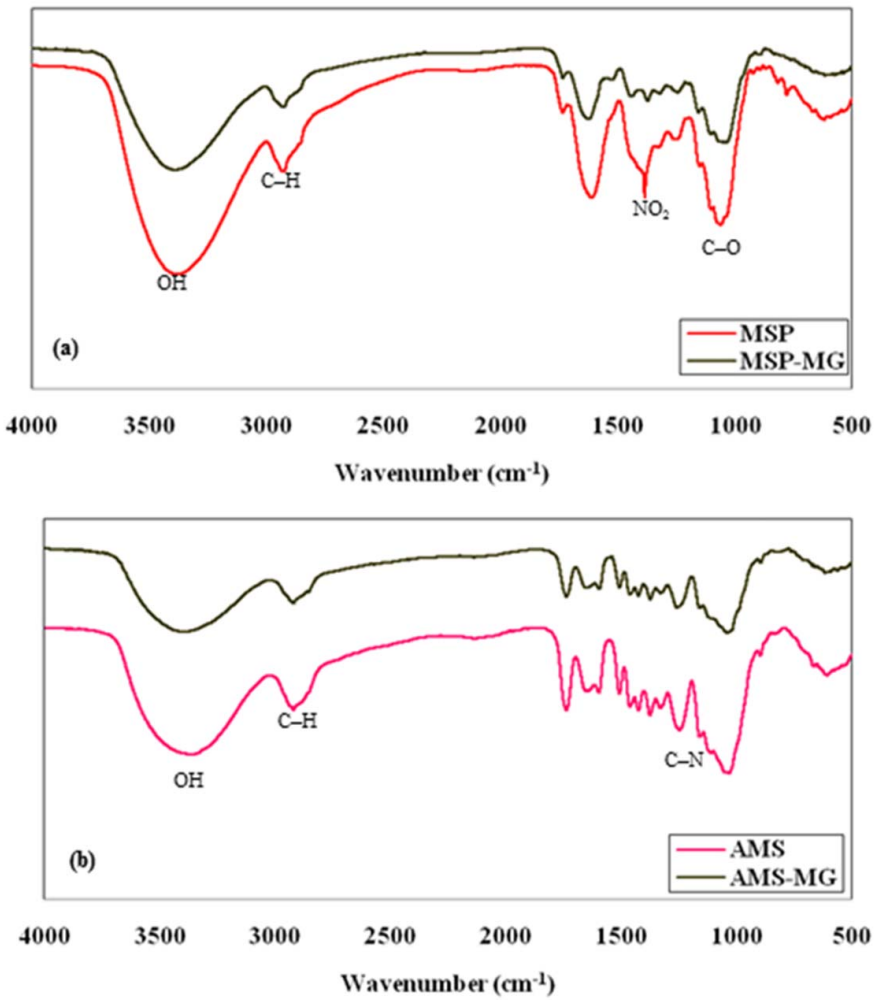

Figure 3. FT-IR spectra of (a) MSP, MG-loaded MSP and (b) AMS, MG-loaded AMS.

MG biosorption on MSP and AMS were showed in Table 4. The Langmuir isotherm model predicted Q_0value of 47.61 mg/g (MSP) and 18.86 mg/g (AMS) revealed good biosorption capacity toward MG removal. The low values of K_L indicated the higher affinity of MG dye molecules with MSP and AMS. The high R^2 values for both the biosorbents showed the better fit of the Langmuir isotherm model with the equilibrium data. As shown in Table 4, the Freundlich isotherm model provided satisfactory fit to the experimental data of MG biosorption using MSP ($R^2 = 0.996$) compared to AMS ($R^2 = 0.978$). The values of n_F of MSP and AMS are found greater than 1.0, indicated the favorable biosorption process. The Jovanovic isotherm model predicted maximum biosorption capacity toward MG removal was found lower than the Langmuir isotherm model. Moreover, the low R^2 values of MSP (0.873) and AMS (0.685) point out that the Jovanovic model cannot describe the biosorption process. Based on the high R^2 value in MSP, Halsey model provides better agreement with the equilibrium biosorption data for MG removal compared to the AMS biosorbent.

All the three-parameter isotherms models considered in the present studied showed higher value of R^2 (Table 4). The low value of Redlich–Peterson constant (B_{RP}) ascertained the model applicability to MG biosorption onto MSP and AMS. The value of Redlich–Peterson model exponent (g) lies between 0 and 1, supported the heterogeneous nature of the MG biosorption process. The Koble-Corrigan isotherm model exponent value (n) were found low for both the biosorbents, suggested that the biosorption surface of MSP and AMS was heterogeneous. The R^2 value of the Sips isotherm model was found highest in both the biosorbents compared to the other two and three parameter isotherm used (Table 4). According to the Sips isotherm model, the biosorption capacity for MG removal using MSP and AMS was found as 111.11 mg/g and 23.80 mg/g, respectively.

Based on the R^2 values, the order of better fitted isotherm models of the MG biosorption equilibrium data using MSP are given as Sips>(Redlich–Peterson, Koble–Corrigan)> (Freundlich, Halsey), Langmuir, Jovanovic. For the MG biosorption using AMS, the better fitted isotherm model given in the following order of Sips > (Langmuir, Koble–Corrigan)> Redlich–Peterson(Freundlich, Halsey), Jovanovic. The results of the biosorption isotherm model showed that the Sips isotherm model best fitted the biosorption data and the Jovanovic isotherm was the least fitted.

Modeling of biosorption kinetics

The kinetic model parameters of pseudo-first-order, pseudo-second-order, Elovich and intraparticle diffusion for the

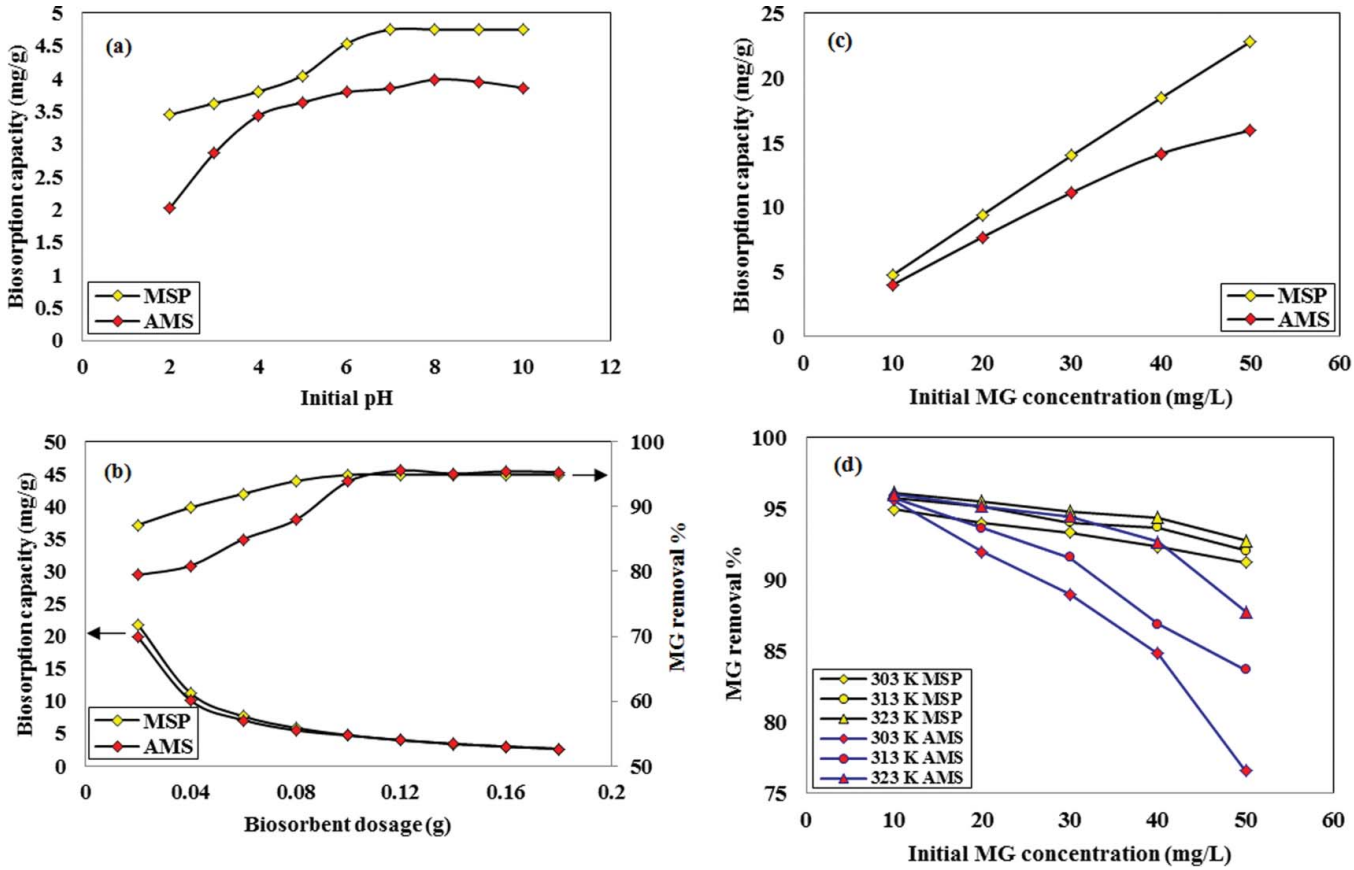

Figure 4. Effects of (a) initial solution pH, (b) biosorbent dosage, (c) initial MG concentration and (d) temperature on the biosorption of MG using MSP and AMS.

biosorption of MG using MSP and AMS are presented in Table 5. Plots obtained for the biosorption experimental data points of pseudo-first-order and Elovich kinetic models not followed the linear regression analysis. The examination of the values of intraparticle diffusion model parameter C was found increased at the higher initial MG concentration resultant in the increase of boundary layer thickness, which in turn enhance the external mass transfer resistance. The low R^2 values of this model represented that additional mechanisms are involved in the MG biosorption process along with intraparticle diffusion. In comparison of all the four kinetic models, the pseudo-second-order model possessed the best fit ($R^2 > 0.997$) with the biosorption experimental data. The pseudo-second-order kinetic model predicted equilibrium biosorption capacity was found higher compared to the other kinetic models predictions. This suggested that the biosorption of MG onto the biosorbents of MSP and AMS was most likely controlled by chemisorption

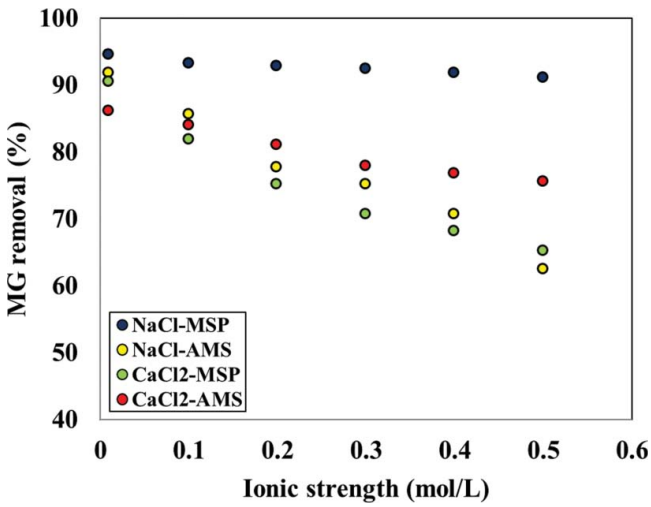

Figure 5. Effect of ionic strength on MG biosorption onto MSP and AMS.

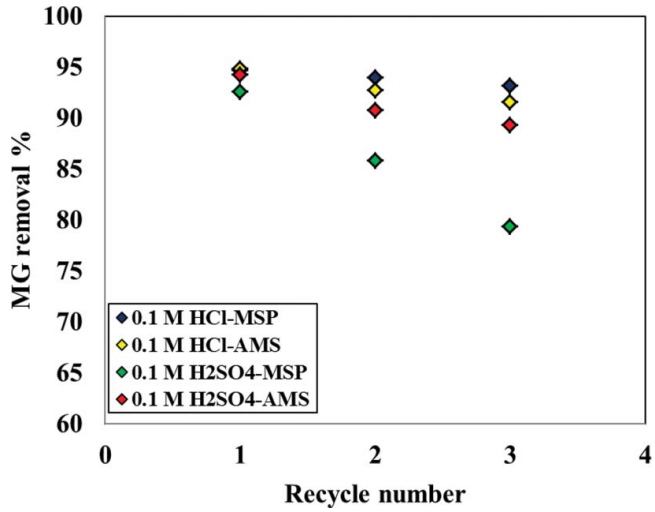

Figure 6. The effect of desorbents on the biosorption efficiency of MSP and AMS toward MG removal up to three cycles.

process, carried out by the valence forces involvement through sharing or electrons exchange between the biosorbents and MG molecules (Oguntimein 2015).

Effect of ion strength on MG biosorption

The dye containing wastewater from the industrial effluents are associated with the presence of different salts. The biosorption process of the MG using MSP and AMS were analyzed in the presence of salts like NaCl, $CaCl_2$ and the concentration ranged from 0.01 to 0.5 M. Figure 5 represents the effect of ionic strength on the biosorption of MG using MSP and AMS. The results showed that the percentage removal of MG decreased as the concentration of NaCl, $CaCl_2$ increased in the biosorption medium from 0.01 to 0.5 M. The presence of NaCl and $CaCl_2$ in the biosorption medium releases Na^+ and Ca^{2+} competes with the MG dye molecules for the active sites on the biosorbents and the possibility of the ion exchange mechanism (Anna 2011).

Biosorbent regeneration

On consideration of cost effective biosorption process, the prepared MSP and AMS were examined for the repeated batch biosorption up to three cycles through the desorption process. The two desorbent solutions of 0.1 M HCl and 0.1 M H_2SO_4 were subjected for the desorption of MG loaded biosorbents. The results of the regeneration studies of the biosorbents were represented in Figure 6. The results showed that 0.1 M HCl employed desorbing agent comparatively showed consistent higher percentage MG removal by MSP and AMS up to three biosorption cycles. The MSP and AMS are potential reusable biosorbents, effectively applied for successive biosorption and desorption process for the removal of MG from aqueous solutions.

Conclusions

The current investigation illustrated the potential use of unconventional lignocellulosic waste biomass MSP and AMS as the low-cost and readily available biosorbents for the sequestration of MG from aqueous solutions. Operating parameters such as initial solution pH, biosorbent dosage, initial MG concentration and temperature were optimized in order to attain the higher biosorption efficiency. The better fit of the isotherm models to the equilibrium data was determined from the coefficient of determination value. The equilibrium data of MSP better fitted with the isotherm models in the following order Sips>(Redlich–Peterson, Koble–Corrigan)>(Freundlich, Halsey), Langmuir, Jovanovic and for AMS was in the order of Sips>(Langmuir, Koble–Corrigan)>Redlich–Peterson(Freundlich, Halsey), Jovanovic, respectively. The intraparticle diffusion was not the only rate controlling step of the MG biosorption process. The calculated thermodynamic parameters showed that the biosorption process was feasible, spontaneous and endothermic nature in the temperature range 303–323 K. The regeneration study showed that HCl was better desorbent agent in both the biosorbents. Therefore, MSP and AMS could be as the potential and cost-effective recyclable biosorbents for the removal of MG from aqueous solutions.

Acknowledgments

The financial support from the Science and Engineering Research Board, Department of Science and Technology, Government of India vide Grant no. PDF/2016/000284 is gratefully acknowledged. The authors are thankful to the National Institute of Technology Rourkela for providing the research facility.

Funding

Science and Engineering Research Board, Department of Science and Technology, Government of India (PDF/2016/000284)

References

Adel AEZ, Nasser SA. 2016. Removal of malachite green dye from aqueous solutions using organically modified hydroxyapatite. J Environ Chem Eng. 4:633–638. doi:10.1016/j.jece.2015.12.014.

Alventosa de Lara E, Barredo Damas S, Alcaina Miranda MI, Iborra Clar MI. 2012. Ultrafiltration technology with a ceramic membrane for reactive dye removal: Optimization of membrane performance. J Hazard Mater. 209–210:492–500. doi:10.1016/j.jhazmat.2012.01.065.

Amin NK. 2008. Removal of reactive dye from aqueous solutions by adsorption onto activated carbons prepared from sugarcane bagasse pith. Desalination. 223:152–161. doi:10.1016/j.desal.2007.01.203.

Anna WK. 2011. Analysis of influence of process conditions on kinetics of malachite green biosorption onto beech sawdust. Chem Eng J. 171:976–985. doi:10.1016/j.cej.2011.04.048.

Bandala ER, Pelaez MA, Garcia-Lopez AJ, Salgado MdJ, Moeller G. 2008. Photocatalytic decolourisation of synthetic and real textile wastewater containing benzidine-based azo dyes. Chem Eng Process. 47:169–176. doi:10.1016/j.cep.2007.02.010.

Dahri MK, Kooh MRR, Lim LBL. 2015. Application of *Casuarina equisetifolia* needle for the removal of methylene blue and malachite green dyes from aqueous solution. Alexandria Eng J. 54:1253–1263. doi:10.1016/j.aej.2015.07.005.

Elhalil A, Tounsadi H, Elmoubarki R, Mahjoubi FZ, Farnane M, Sadiq M, Abdennouri M, Qourzal S, Barka N. 2016. Factorial experimental design for the optimization of catalytic degradation of malachite green dye in aqueous solution by Fenton process. Water Resour Ind. 15:41–48. doi:10.1016/j.wri.2016.07.002.

Freundlich HMF. 1906. Uber die adsorption in losungen. Z Phys Chem (Leipzig). 57A:385–470.

Fumihiko O, Daisuke I, Naohito K. 2015. Cationic dye removal from aqueous solution by waste biomass produced from calcination treatment of rice bran. J Environ Chem Eng 3:1476–1485. doi:10.1016/j.jece.2015.05.025.

Halsey G. 1948. Physical adsorption on nonuniform surfaces. J Chem Phys. 16:931–937. doi:10.1063/1.1746689.

Ho YS, McKay G. 1999. Pseudo-second order model for sorption processes. Process Biochem. 34:451–465. doi:10.1016/S0032-9592(98)00112-5.

Jovanovic DS. 1969. Physical adsorption of gases I: isotherms formonolayer and multilayer adsorption. Colloid Polym Sci. 235:1203–1214.

Kaur R, Kaur H. 2017. *Calotropis procera* an effective adsorbent for removal of Congo red dye: Isotherm and kinetics modelling. Model Earth Syst Environ. doi: 10.1007/s40808-017-0274-3.

Koble RA, Corrigan TE. 1952. Adsorption isotherms for pure hydrocarbons. Ind Eng Chem. 44:383–387. doi:10.1021/ie50506a049.

Kumar SS, Balasubramanian P, Swaminathan G. 2013. Degradation potential of free and immobilized cells of white rot fungus *Phanerochaete chrysosporium* on synthetic dyes. Int J Chem Tech Res 5:565–571.

Lagergren S. 1898. About the theory of so-called adsorption of soluble substances, K. Svenska Vetenskapsakad. Handl. 24:1–39.

Langmuir I. 1918. The adsorption of gases on plane surfaces of glass, mica and platinum. J Am Chem Soc. 40:1361–1403. doi:10.1021/ja02242a004.

Lin KYA, Chang HA. 2015. Ultra-high adsorption capacity of zeolitic imidazole framework-67 (ZIF-67) for removal of malachite green from water. Chemosphere. 139:624–631. doi:10.1016/j.chemosphere.2015.01.041.

Liu M, Liu Z, Yang T, He Q, Yang K, Wang H. 2017. Studies of malachite green adsorption on covalently functionalized Fe_3O_4@SiO_2–graphene oxides core–shell magnetic microspheres. J Solgel Sci Technol. DOI: 10.1007/s10971-017-4307-1.

Mustafa TY, Tushar KS, Sharmeen A, Ang HM. 2014. Dye and its removal from aqueous solution by adsorption: A review. Adv Colloid Interface Sci. 209:172–184. doi:10.1016/j.cis.2014.04.002.

Oguntimein GB. 2015. Biosorption of dye from textile wastewater effluent onto alkali treated dried sunflower seed hull and design of a batch adsorber. J Environ Chem Eng. 3:2647–2661. doi:10.1016/j.jece.2015.09.028.

Rajesh Kannan R, Rajasimman M, Rajamohan N, Sivaprakash B. 2010. Brown marine algae turbinaria conoides as biosorbent for Malachite green removal: Equilibrium and kinetic modeling. Front Environ Sci Eng China. 4:116–122. doi:10.1007/s11783-010-0006-7.

Rangabhashiyam S, Anu N, Selvaraju N. 2013a. The significance of fungal laccase in Textile Dye Degradation—A Review. Res J Chem Environ. 17:88–95.

Rangabhashiyam S, Anu N, Giri Nandagopal MS, Selvaraju N. 2014b. Relevance of isotherm models in biosorption of pollutants by agricultural byproducts. J Environ Chem Eng. 2:398–414. doi:10.1016/j.jece.2014.01.014.

Rangabhashiyam S, Anu N, Selvaraju N. 2013b. Sequestration of dye from textile industry wastewater using agricultural waste products as adsorbents. J Environ Chem Eng. 1:629–641. doi:10.1016/j.jece.2013.07.014.

Rangabhashiyam S, Suganya E, Selvaraju N, Lity AV. 2014a. Significance of exploiting non-living biomaterials for the biosorption of wastewater pollutants. World J Microbiol Biotechnol. 30:1669–1689. doi:10.1007/s11274-014-1599-y.

Rangabhashiyam S, Sujata Lata, Balasubramanian P. 2017. Biosorption characteristics of methylene blue and malachite green from simulated wastewater onto *Carica papaya* wood biosorbent. Surf Interfaces https://doi.org/10.1016/j.surfin.2017.09.011

Redlich O, Peterson DL. 1959. A useful adsorption isotherm. J Phys Chem. 63:1024. doi:10.1021/j150576a611.

Shirmardi M, Mahvi AH, Hashemzadeh B, Naeimabadi A, Hassani G, Niri MV. 2013. The adsorption of malachite green (MG) as a cationic dye onto functionalized multi-walled carbon nanotubes. Korean J Chem Eng. 30:1603–1608. doi:10.1007/s11814-013-0080-1.

Sips RJ. 1948. On the structure of a catalyst surface. J Chem Phys. 16:490–495. doi:10.1063/1.1746922.

Srivastava S, Sinha R, Roy D. 2004. Toxicological effects of malachite green. Aquat Toxicol. 66:319–329. doi:10.1016/j.aquatox.2003.09.008.

Sushmita B, Gopesh CS, Ravindra KG, Chattopadhyaya MC, Siddh NU, Yogesh CS. 2016. Removal of malachite green, a hazardous dye from aqueous solutions using *Avena sativa* (oat) hull as a potential adsorbent. J Mol Liq. 213:162–172. doi:10.1016/j.molliq.2015.11.011.

Tzvetkov G, Mihaylova S, Stoitchkova K, Tzvetkov P, Spassov T. 2016. Mechanochemical and chemical activation of lignocellulosic material to prepare powdered activated carbons for adsorption applications. Powder Technol. 299:41–50. doi:10.1016/j.powtec.2016.05.033.

Vijayaraghavan K, Rangabhashiyam S, Ashokkumar T, Arockiaraj J. 2017. Assessment of samarium biosorption from aqueous solution by brown macroalga *Turbinaria conoides*. J Taiwan Inst Chem Eng. 74:113–120. doi:10.1016/j.jtice.2017.02.003.

Wang XS. 2010. Invasive freshwater macrophyte alligator weed: novel adsorbent for removal of malachite green from aqueous solution. Water Air Soil Pollut. 206:215–223. doi:10.1007/s11270-009-0097-6.

Weber WJ, Morris JC. 1962. Advances inwater pollution research: removal of biologically resistant pollutants from waste waters by adsorption, Proceedings of International Conference on Water Pollution Symposium; Pergamon Press, Oxford 2:231–266.

Wu FC, Tseng RL, Juang RS. 2009. Characteristics of Elovich equation used for the analysis of adsorption kinetics in dye-chitosan systems. Chem Eng J 150:366–373. doi:10.1016/j.cej.2009.01.014.

Zeng G, Cheng M, Huang D, Lai C, Xu P, Wei Z, Li N, Zhang C, He X, He Y. 2015. Study of the degradation of methylene blue by semi-solid-state fermentation of agricultural residues with *Phanerochaete chrysosporium* and reutilization of fermented residues. Waste Manag. 38:424–430. doi:10.1016/j.wasman.2015.01.012.

Zhou L, Ma J, Zhang H, Shao Y, Li Y. 2015. Fabrication of magnetic carbon composites from peanut shells and its application as a heterogeneous Fenton catalyst in removal of methylene blue. Appl Surface Sci. 324:490–498. doi:10.1016/j.apsusc.2014.10.152.